

1 **Natural or anthropogenic? On the origin of atmospheric** 2 **sulfate deposition in the Andes of South Eastern Ecuador**

3

4 ***S. Makowski Giannoni 1, R. Rollenbeck1, K. Trachte1 and J. Bendix1***

5 [1] {Laboratory for Climatology and Remote Sensing (LCRS), Faculty of Geography, University
6 of Marburg, Deutschhausstr. 12, D-35032 Marburg, Germany}

7 Correspondence to: S. Makowski Giannoni (sandro.makowski@posteo.org)

8

9 **Abstract**

10 Atmospheric sulfur deposition above certain limits can represent a threat to tropical forests,
11 causing nutrient imbalances and mobilizing toxic elements that impact biodiversity and forest
12 productivity. Atmospheric sources of sulfur deposited by precipitation have been roughly
13 identified in only a few lowland tropical forests. Even scarcer are these type of studies in tropical
14 mountain forests, many of them megadiversity hotspots and especially vulnerable to acidic
15 deposition. Here, the topographic complexity and related streamflow conditions affect the origin,
16 type, and intensity of deposition. Furthermore, in regions with a variety of natural and
17 anthropogenic sulfur sources, like active volcanoes and biomass-burning, no source-emission
18 data has been used for determining the contribution of each of them to the deposition. The main
19 goal of the current study is to evaluate sulfate (SO_4^-) deposition by rain and occult precipitation at
20 two topographic locations in a tropical mountain forest of southern Ecuador, and to trace back the
21 deposition to possible emission sources applying back trajectory modeling. To link upwind
22 natural (volcanic) and anthropogenic (urban/industrial and biomass-burning) sulfur emissions and
23 observed sulfate deposition, we employed state of the art inventory and satellite data, including
24 volcanic passive degassing as well. We conclude that biomass-burning sources generally
25 dominate sulfate deposition at the evaluated sites. Minor sulfate transport occurs during the
26 shifting of the predominant winds to the north and west. Occult precipitation sulfate deposition
27 and likely rain sulfate deposition are mainly linked to biomass-burning emissions from the
28 Amazon lowlands. Volcanic and anthropogenic emissions from the north and west contribute to
29 occult precipitation sulfate deposition at the mountain crest *Cerro del Consuelo* meteorological

1 station and to rain-deposited sulfate at the upriver mountain-pass *El Tiro* meteorological station.

2

3 **1 Introduction**

4 Sulfur enters the atmosphere principally as sulfur dioxide (SO₂), an air pollutant with a lifetime of
5 about one to two days, before it is normally deposited or oxidized to sulfate (SO₄). After
6 oxidation, lifetime increases to three or more days, depending on the state of the atmosphere and
7 the injection height. Because of its longer life time, sulfate can be spread over greater distances.
8 In high concentrations, sulfate decreases the pH of precipitation to levels that represent a threat to
9 health and ecosystems. This phenomenon called “acid rain” was discussed in the past,
10 particularly in the industrialized countries of Europe and North America where adverse effects
11 were found to be more serious for health than for ecosystems (Menz and Seip, 2004).

12 In tropical ecosystems, only a few studies are available despite the fact that they are mostly
13 characterized by an interference-prone biogeochemical cycle and nutrient limitation (Elser et al.,
14 2007; Wullaert et al., 2010), and hence particularly sensitive to acid deposition (Boy et al., 2008;
15 Delmelle et al., 2002). Kuylenstierna et al. (2001), for example, revealed that acidification from
16 atmospheric sulfur could represent a threat to tropical ecosystems in developing countries.
17 Acidification of soils due to persistent increase in sulfate inputs could lead to nutrient imbalances
18 and changes in ecosystem diversity and productivity (Greaver et al., 2012; Phoenix et al., 2006).
19 It can also mobilize many potentially toxic elements that promote soil degradation and erosion in
20 some areas. Acid and toxic elements can leach out of the soil by rain and go into ground waters
21 and nearby water-bodies (Ljung et al., 2009). Considering these adverse effects of acidic
22 deposition in land ecosystems, serious impacts can be expected, especially in highly biodiverse
23 and disturbance-sensitive forest ecosystems. The latter becomes much more likely if we add that
24 emissions and related deposition in developing countries are rapidly increasing, and that 50–80%
25 of the fraction of deposition on land falls on natural vegetation and not close to the sources
26 (Dentener et al., 2006).

27 Regarding the sources of deposition, SO₂ is emitted from different natural and anthropogenic
28 processes. Volcanoes are considered the most important natural sources representing around 26-
29 35% of total global emissions (Graf et al., 1997; Stevenson et al., 2003). The most important
30 anthropogenic sources are fossil fuel combustion from energy production, transportation, and

1 industrial activity in big cities and their hinterlands, and biomass-burning from deforestation,
2 land clearing, and bush fires (Lee et al., 2011; Smith et al., 2011). The contribution of each to the
3 total SO₂ emissions may vary in accordance to the region and its development state (industrial or
4 industrializing countries). However, in some tropical regions (e.g. Ecuador) volcanic emissions
5 and biomass-burning might contribute larger amounts in consequence of the density of active
6 volcanoes (Carn et al., 2008) and an accelerated land use change mostly characterized by
7 deforestation to gain arable land (Crutzen and Andreae, 1990; Rudel et al., 2005).

8 On a local to regional scale, detailed knowledge on pollutant deposition from rain and cloud
9 water in specific regions, its sources, and its smaller-scale spatial variability, particularly in
10 complex terrain as that of the Andes, is still scarce. To date, only few studies on atmospheric
11 acidic deposition exist for tropical ecosystems and those including a characterization of source
12 emissions are very rare.

13 Precipitation chemistry surveys in some montane but mainly lowland tropical forests of Costa
14 Rica, Venezuela, Puerto Rico, Cameroon, and Brazil have characterized nutrient and pollutant
15 deposition by analyzing ionic concentrations, among others sulfate, and in situ meteorological
16 parameters. In Venezuela and Cameroon, Morales et al. (1998) and Sigha-Nkamdjou et al. (2003)
17 indicated the relative importance of local sources, such as biogenic sulfur oxidation by swamps
18 and lakes, to sulfate deposition. However, industrial emissions were indicated as the most
19 important source of sulfate deposition in Venezuela. The opposite was found by Eklund et al.
20 (1997) and Gordon et al. (1994) in Costa Rica and Puerto Rico, respectively, where no significant
21 pollution footprints were found in the samples of the two studied tropical mountain forests. The
22 same was noticed by Pauliquevis et al. (2012) in the central Amazon of Brazil, where high sulfate
23 loads in rain water likely stem from the oxidation of sulfur compounds from the Atlantic Ocean.

24 In areas with an important number of active volcanoes like Indonesia, Costa Rica, and Nicaragua,
25 volcanic emissions were given special attention as contributors of acidic sulfate deposition in the
26 surrounding areas and downwind of the emitting craters (Delmelle et al., 2001, 2002; Langmann
27 and Graf, 2003; Pfeffer et al., 2006). For Central Africa and tropical South America, however,
28 emissions from burning forests, savannas, and agricultural fields were claimed as the principal
29 source of atmospheric pollution (Hansen et al., 2013; Rissler et al., 2006; van der Werf et al.,
30 2010) and reactive sulfur deposition in the downwind regions (Diehl et al., 2012; Fabian et al.,
31 2005).

1 With regard to the megadiverse tropical mountain rainforest in the south-eastern Ecuadorian
2 Andes (Bendix and Beck, 2009), biomass-burning in the Amazon has been hitherto identified as
3 the principal source of atmospheric sulfate deposition (Beiderwieden et al., 2005; Boy et al.,
4 2008; Fabian et al., 2005, 2009; Rollenbeck et al., 2011). However, volcanic and biomass-
5 burning emissions were included by roughly estimated data. Given the dense concentration of
6 active volcanoes in Ecuador, where as much as 95% of emissions can stem from non eruptive
7 degassing, and considering the difference in emissions between burned areas depending on land
8 use type, it is of utmost importance to include data on source emissions as accurately as possible
9 to characterize air-mass pollution history leading to the deposition. Furthermore, preliminary
10 work on nitrogen deposition has shown that crest areas considerably differ in their behavior from
11 valley sites (Makowski Giannoni et al., 2013). Hence, a comprehensive deposition analysis must
12 not only investigate sinks and source intensities but should also study different topographic
13 positions.

14 Consequently, the main aim of the current study is (1) to determine sulfate deposition at two
15 different topographic positions in the mountain rain forest of southern Ecuador and (2) to trace
16 back the deposition to different natural and anthropogenic emission sources applying back
17 trajectory modeling. To link the spatio-temporal patterns of upwind natural (volcanoes) and
18 anthropogenic (urban/industrial and biomass-burning) sulfur emissions to sulfate deposition at
19 site, we used the latest state of the art inventories and satellite data, also considering volcanic
20 passive degassing.

21

22 **2 Geographical setting**

23 The Reserva Biológica San Francisco (RBSF) (4°00 S and 79°00 W) is located in a remote area
24 at the outer edge of the Amazon, on the eastern slopes of the South Ecuadorian Andes, between
25 the humid Amazon plains and the dryer interandean valleys. The RBSF lies within the small San
26 Francisco River catchment between the capital cities of Loja and Zamora (Fig. 1). The protected
27 forest and the pastures outside of the reserve have been subject of investigations from two
28 successive multidisciplinary research groups funded by the German Research Council (DFG)
29 since 2002 (Beck et al., 2008; Bendix et al., 2013). The terrain height of the area is lower
30 compared to the northern and southern Andes and its topography more complex, as the system of

1 few parallel mountain ranges gives way to a net of small valleys and cordilleras (Rollenbeck et
2 al., 2011).

3 There are only a few sources of pollution in the vicinity of the RBSF. The cities of Loja (~214
4 855 inhabitants, 10 km to the west; (INEC), 2010) and Zamora (~25 510 inhabitants, 14 km
5 south-east; (INEC), 2010) are quite small and without any notable industrial activity. Between
6 October and December, a relative dry season, slash and burn is a common practice in local
7 pasture management which quite often runs out of control, burning adjacent areas of forest
8 (Bendix et al., 2008b; Curatola Fernández et al., 2013; Hartig and Beck, 2003).

9 The synoptic winds at the upper levels of the cordillera consist of tropical easterly trades over
10 more than 70% of the time. North-easterlies prevail between January and March while south-
11 easterlies dominate between June and September. The remaining 30% corresponds to westerlies
12 and northerlies, mainly occurring between end October and December (Bendix et al., 2008a;
13 Emck, 2007).

14 Precipitation varies, mainly depending on the migration of the Inter Tropical Convergence Zone
15 (ITCZ) and the variation in the direction of the tropical easterlies. The associated humidity
16 advection dominates the amount of atmospheric water entering the ecosystem. The total annual
17 average of rainfall (rainfall and occult precipitation) range from 1850 to 6300 mm year-1 along
18 an altitudinal gradient between 1960 and 3180 m.a.s.l.. Occult precipitation (OP) frequencies of
19 up to 85% of the time particularly occur in the more elevated parts of the research area, when
20 warm and humid air masses from the Amazon lowlands hit the Andes, leading to intense
21 condensation and clouds immersion (Bendix et al., 2006a, 2006b; Emck, 2007; Rollenbeck,
22 2010).

23

24 **3 Data and methods**

25 In the present study we discuss the variation of sulfate concentration/deposition in precipitation in
26 a five year period (2005-2009) at two meteorological Stations (MSs). Higher locations are more
27 vulnerable to higher deposition (Makowski Giannoni et al., 2013), hence the selection of the two
28 highest MSs in the RBSF for this study. Because of the strong winds at the locations of sampling,
29 we will refer to all type of light precipitation, from wind-driven drizzle down to fog and cloud

1 droplets as OP.

2 For studying source-receptor relationships we brought together measurements of sulfate
3 concentrations in rain and OP samples with backtrajectory transport modeling using satellite and
4 emission inventories as inputs. The modeling of SO₂ transport, hereinafter referred to as “SO₂
5 transport”, results in SO₂ daily concentration values at the target coordinates, which match the
6 observation sites.

7 The following subsections (3.1-3.2) are devoted to a detailed description of the data and methods
8 used. The last subsection (3.2.2) mentions and discusses the techniques employed to unveil the
9 relationships between in-situ observations and transport to the observation sites.

10 3.1 Data

11 3.1.1 Sulfate in rain and OP

12 We measured rainfall and OP at two MSs: one installed on the highest surrounding peak (*Cerro*
13 *del Consuelo*, 3180 m.a.s.l.) and the other one on a mountain pass upriver (*El Tiro*, 2870 m.a.s.l.),
14 separating the basin of Loja in the west from the eastern slopes of the Andean mountain range
15 (Fig. 1).

16 The collection of samples was conducted on a weekly basis between 2005 and 2009. Rain was
17 sampled using UMS-RS 200 polyethylene rain samplers of 20 cm diameter. Standard fog
18 collectors (Schemenauer and Cereceda, 1994) were used to sample OP. With a size of 1 x 1 m
19 and composed of polypropylene nets with a 2 x 1 mm mesh width, they were set up at 90° with
20 respect to the main wind direction and collect all type of deposition, as particles, aerosols, and
21 gases (Fabian et al., 2005).

22 We did not use wet-only collectors, so dry deposition is likely adding to the total deposition. For
23 the fog collectors, Schemenauer et al. (1995) estimated the contribution of dry deposition to the
24 total deposition to be less than 5 % for temperate mountain forests of North America. Because of
25 the very humid conditions in our study site (high frequency of cloud immersion, around 85 % of
26 the time, Bendix et al. 2008a), and the dense vegetation cover, which implies no sources for
27 turbulent generation of local aerosol, dry deposition's contribution is most probably irrelevant for
28 fog collectors (very probably less than that found by Schemenauer et al., 1995) and rain gauges.
29 Considering that one of our goals is to evaluate sulfate inputs into the ecosystem, the catching

1 efficiency from collectors in relation to trees is also an important parameter. For this
2 Schemenauer and Cerceda (1994) found good agreements between collection rates of different
3 tree species and the standard fog collectors that we used in this study. For further details on field
4 measurement techniques, calibration, and handling of the data the reader is referred to Fabian et
5 al. (2005) and Rollenbeck et al. (2007, 2011). On the day of collection, electrical conductivity
6 (WTW-LF 90) and pH (Methron 73065/682) of the samples were measured on site. Then, the
7 samples were stored deep frozen until chemical analyses were carried out.

8 Ion chromatography (Dionex DX-210) was used to measure concentrations of sulfate ions in rain
9 and OP water. The sulfate ions were taken as proxies of sulfur inputs into the ecosystem. Finally,
10 time series of sulfate volume weighted monthly mean (VWMM) concentrations and total
11 deposition rates in rain and OP water were created for the period 2005-2009.

12 **3.1.2 SO₂ source data**

13 We used three recent emission inventories and one satellite dataset as emission inputs to simulate
14 the SO₂ transport to our study area: (a) one for anthropogenic emissions (EDGARv4, Janssens-
15 Maenhout et al., 2012), (b) one for biomass-burning (GFEDv3, Mu et al., 2011) and (c) one for
16 emissions from volcanic degassing and explosive eruptions (Aerocom, Diehl et al., 2012). The
17 ozone monitoring instrument (OMI) SO₂ data accounts mostly for SO₂ emissions from volcanoes,
18 including passive degassing, but very strong anthropogenic pollution events are also detected by
19 the sensor (Carn et al., 2007, 2008).

20 (a) The emissions in EDGARv4 are calculated using a technology based emission factor
21 approach which includes country-specific emissions when these are available. Emissions are
22 allocated spatially on a 0.1 x 0.1 degree grid cells for point, line, and area sources built upon
23 geographic datasets such as the location of energy and manufacturing facilities, road networks,
24 and population density. In version 4 EDGAR delivers now annual emission estimates from 1970
25 to 2008, which represents an advantage compared to former static inventories. For more
26 information readers may visit the EDGAR website (<http://edgar.jrc.ec.europa.eu/index.php>).

27 (b) For biomass-burning SO₂ estimates, we used the GFEDv3 inventory. The compilation of this
28 inventory was based on a biogeochemical model (CASA-GFED) that approximates fuel loads
29 and combustion completeness for each time-step, and burned area data from satellite observations
30 (van der Werf et al., 2010). Considering that fires and volcanic eruptions are very often sporadic

1 and transient, the high temporal and spatial resolution appear very advantageous when dealing
2 with the variation of emissions in space and time. Some issues which might reduce the regional
3 quality are the underestimation of emissions in the tropics because of cloud cover and canopy
4 closeness, and gaps in the satellite coverage.

5 (c) As part of the AeroCom global emission inventories, a daily-resoluted volcanic SO₂ emission
6 dataset was generated for the time period 1979-2009 including all volcanoes with historic
7 eruptions listed in the Global Volcanism Program (<http://www.volcano.si.edu/>). Since volcanic
8 emissions are in some cases occasional, the high temporal resolution of the inventory is
9 indispensable for capturing the variability in the emission rates. Emissions for 1167 volcanoes
10 considered to be active were compiled. The emissions originating from passive and quiescent
11 degassing are also taken into account. The default SO₂ estimates are based on the Volcanic Sulfur
12 Index (VSI). In cases where data from the total ozone mapping spectrometer (TOMS), OMI or
13 the correlation spectrometer (COSPEC) were available the respective values were replaced by
14 emissions calculated from these observations. In other cases the default values were replaced by
15 more precise estimations from the literature. For more information on the AeroCom volcanic SO₂
16 inventory readers are referred to Diehl et al. (2012) and the AeroCom website
17 (<http://aerocom.met.no/emissions.html>).

18 The OMI on board the polar-orbiting AURA satellite is a nadir solar backscatter spectrometer
19 with a spatial footprint of 13 x 24 km that spans the earth surface in one day. The instrument's
20 UV-2 channel, which is used for the SO₂ retrievals, has a mean spectral resolution of 0.45 nm.
21 Both, its spatial and spectral resolution, as well as its daily global coverage allows for a SO₂
22 retrieval based monitoring of low emission sources like volcanic passive degassing and smelter
23 plumes which was not possible with former instruments like TOMS or GOME. OMI SO₂ data
24 was already successfully applied for daily monitoring of volcanic degassing in Ecuador (Carn et
25 al., 2008) and the detection of SO₂ emissions from Peruvian copper smelters (Carn et al., 2007).
26 Although the OMI instrument cannot distinguish between anthropogenic and volcanic SO₂ when
27 co-occurring in close vicinity, Carn et al. (2007) concluded that anthropogenic sources in the
28 coastal plains of Ecuador would only contribute to less than 1% to the total amount measured by
29 OMI. In the current study, we used subsets of the OMI data replicating the same geographical
30 domain defined by Carn et al. (2008) for Ecuadorian volcanic emissions. The region selected is
31 not affected by the South-Atlantic anomaly, an artifact impacting on the retrievals of a big area in

1 central and southern South America (Lee et al., 2011), which means that OMI retrievals are
2 reliable in the selected domain. The concentration retrieved by OMI was assumed to represent
3 mainly the Ecuadorian volcanic emission's contribution to the atmospheric SO₂ concentrations.
4 Given its small geographic domain, the OMI data is set to account for regional emissions from
5 Ecuador and southern Colombia.

6 **3.2 Methods**

7 **3.2.1 Trajectory modeling**

8 To link potential SO₂ source regions with the sulfate concentration measurements in our study
9 site, a tool was developed which models the transport of SO₂ from upwind sources (biomass-
10 burning, anthropogenic, and volcanic emissions) to our receptor area. The tool follows the path of
11 the trajectories and adds the emission amounts from the pixels that prove spatial and temporal
12 coincidence until a target point which corresponds to the coordinates of the RBSF. No chemical
13 or physical transformations are included in the modeling scheme. Scavenging and rain-out
14 processes are accounted for by a decay function integrated into the algorithm. For more details on
15 the tool refer to Rollenbeck (2010) and Makowski Giannoni et al. (2013).

16 **3.2.2 Observation and model data processing and evaluation**

17 To calculate best estimates of precipitation (rain and OP), we used a method similar to the one
18 used in the Goddard Institute for Space Studies Surface Temperature Analysis (GISTEMP,
19 Hansen et al., 2010). Nearby MSs were used to evaluate unrealistic values and to fill-in data gaps
20 of the MSs that we used in this study.

21 Time series of volume-weighted Conductivity and pH monthly means were compiled and
22 summary statistics as median, median absolute deviation (MAD), and minimum and maximum
23 values calculated. For sulfate concentrations in both types of precipitation VWMM were also
24 calculated and time-series covering the whole observation period were built. Here we identified
25 the time span in which peak values or regular phenomena took place, as well as long term trends.
26 All time-series were then compared to check for acidification of the samples when highly loaded
27 with sulfate ions.

28 Additionally, we calculated and analyzed annual mean deposition rates for *El Tiro* and *Cerro del*

1 *Consuelo* MSs to have a measure of sulfate input variability per unit area, which is of importance
2 for assessing potential impacts on ecosystems by a Nutrient Manipulation Experiment (NUMEX,
3 Homeier et al. 2012).

4 For source-receptor analysis the daily transport model outputs were first aggregated according to
5 the dates of sample collection in the field, in order to achieve comparable values for time-series
6 compilation and correlation analysis. We calculated the mean weekly values to compensate for
7 irregular time intervals between collection of samples. We then used these new values to
8 calculate SO₂ transport monthly averages and to compile transport time-series from the different
9 emission sources represented by the emission inventories and satellite data. Before proceeding
10 with statistical analysis, all the data was transformed to a logarithmic scale to approach
11 normality. We then carried out a Pearson correlation analysis to test for correlations between field
12 observations (VWMM sulfate concentrations) and model outputs (SO₂ transport); we used
13 VWMM and not deposition values to avoid extra uncertainty added by new variables present in
14 the deposition calculations. Finally, visual analysis of coincidences between transport and
15 VWMM concentration time-series was performed, taking into account events which could
16 influence the transport of sulfate and its deposition into our study area.

17 In addition to the bivariate correlation analysis, we applied a factor analysis with varimax rotation
18 to test for variance explanation from groups of variables.

19

20 **4 Results**

21 **4.1 Emission sources and annual deposition**

22 The highest precipitation and OP inputs were registered from April to July at *Cerro del*
23 *Consuelo* MS (Fig.2a), and in February and from April to June, at *El Tiro* MS (Fig.2b). A short
24 dry season took place between September and November. Rain quantity varied significantly
25 between dry and wet periods while OP inputs remained quite constant at around 100 mm for both
26 MSs over the whole observation period.

27 The calculated volume-weighted monthly pH values in samples from *Cerro del Consuelo* MS
28 yielded median values of 5.3 and 5 with a median absolute deviation (MAD) of 0.36 and 0.29 in
29 rain and OP, respectively (Tab. 1). The water samples in both types of precipitation input tended

1 to be acidic with some extreme values going as low as 1.86 in OP samples and 3 in rain samples.
2 OP sulfate concentration presented a negative, weak but significant correlation with pH values
3 (Pearson, $r = -0.34$, $p < 0.05$). Conductivity values ranged between 1.4 and 72 S/m, with median
4 values of 2.6 and 8.1 S/m in OP and rain, respectively. The bulk of the data ranged, nevertheless,
5 between 1.4 and 14.3 S/m. Conductivity is a proxy of ion concentrations in water and thus, high
6 conductivity values coincide with episodes of highly ion-loaded rain and OP water droplets.

7 In samples from *El Tiro* MS, pH volume-weighted values were in the acidic area of the spectrum
8 too, with median values of 5.4 and 4.8 and MAD of 0.51 and 0.37 in rain and OP, respectively
9 (Tab. 1). There was a strong negative correlation between sulfate concentration in OP and pH
10 (Pearson, $r = -0.64$, $p < 0.001$), and a weaker one for sulfate concentration in rain (Pearson, $r =$
11 -0.34 , $p < 0.05$). Median conductivity values were generally higher when compared to those at
12 *Cerro del Consuelo* MS. They yielded a median of 10.9 and 3.7 S/m in OP and rain, respectively.
13 Opposed to what we observed at *Cerro del Consuelo* MS, conductivity was much higher in OP
14 than in rain at *El Tiro* MS, meaning a strong ion load; values ranged between 1.4 and 110.3 S/m.

15

16 Figure 3 shows the annual sulfate deposition by rain and OP at (a) *Cerro del Consuelo* and (b) *El*
17 *Tiro* MSs. The deposition was generally higher for *Cerro del Consuelo* MS for both types of
18 precipitation. The only exception was the year 2009 where the OP deposition at *El Tiro* MS
19 increased significantly in comparison to a decrease at *Cerro del Consuelo*. The highest amount of
20 sulfate was deposited by rain in 2007 at the *Cerro del Consuelo* MS. Lowest burden was
21 observed in rain samples from *El Tiro* MS in 2009. The figure shows that *El Tiro* MS was
22 experiencing higher annual deposition rates by OP nearly over all years, pointing to a more
23 advective environment. In contrary, *Cerro del Consuelo* MS was characterized by changing
24 deposition maxima between rain and OP over time.

25 A tendency towards lower OP sulfate deposition (light grey bars) was observed in Fig. 3, with an
26 upturn in 2009 for *El Tiro* MS. Deposition by rain (dark grey bars) was more oscillating,
27 especially in the quantities deposited at *Cerro del Consuelo* MS. A negative tendency in rain
28 deposition was clearer since 2008.

29 Concerning the emissions, Fig. 4 depicts five year average maps of emissions for every dataset
30 used for simulating transport. From a rather local perspective, emissions from volcanoes

1 appeared to be intense mainly close to the most active volcanoes: *Sangay*, *Tungurahua* and
2 *Reventador* (Fig. 4a). Emissions from big cities only seemed to be evident for the metropolitan
3 region of Guayaquil and Quito, but much seems contaminated with SO₂ emissions from
4 volcanoes, which plumes were transported principally to the west and south west and cover part
5 of the ocean next to the southern coast of the country. The strong emissions east of *Reventador*
6 most probably have its origin in deforestation activity. The high emission pixels at the same
7 location in the biomass-burning dataset (Fig. 4c) support this argument.

8 Figure 4b show volcanic emissions from eruptions and passive degassing. Once again, *Sangay*,
9 *Tungurahua*, and *Reventador* belong to the volcanoes that contribute the most to the emissions in
10 Ecuador. In Colombia, *Nevado del Huila* and *Galeras* are the strongest SO₂ emitters. For
11 biomass-burning, the main region is located in the Brazilian and Bolivian Amazon (Fig. 4c). The
12 Venezuelan savanna in the north-east is another important biomass-burning region. The majority
13 of potential anthropogenic sources (industrial, urban, and transportation) are located in the north
14 of our study area (Fig. 4d). This occurs owing to the extremely scarce significant sources in the
15 east and because no air masses arriving to our study area originate and pass over the sources in
16 the south.

17 **4.2 Linking emissions to deposition**

18 **4.2.1 Correlation analyses**

19 A first test, using a cross-correlation technique, is required to unveil the dependence of the
20 transport data sets. This is shown in Tab. 2. Only moderate relations for *El Tiro* and somewhat
21 higher correlations for *Cerro del Consuelo* were revealed by this analysis. As expected, volcanic
22 and anthropogenic source concentrations correlate well while only low (partly negative)
23 correlations between biomass-burning and anthropogenic and volcanic pollutant transport is
24 visible. This means that there is some overlap in the data sets related to volcanic and
25 anthropogenic emissions. The negative correlation between anthropogenic and biomass-burning
26 could indicate that their transport depends on changing wind direction (east for biomass-burning,
27 north and west for anthropogenic) which means that the anthropogenic sources affecting the area
28 are located more in the western and northern sectors.

29 To connect sinks with sources, correlation analysis between atmospheric SO₂ concentration in the

1 pixel representing the location of the observation site, derived by back-trajectory modeling, and
2 the measured sulfate concentrations was conducted. Pearson's correlation coefficients calculated
3 for sulfate concentration and SO₂ transport are presented in Tab. 3. It is observed that, even if
4 significant, the correlations between source and sink data are generally low.

5 For *Cerro del Consuelo* crest site it is interesting to see that more evident correlations occur
6 between OP and volcanic emissions. Because OMI includes volcanic emissions, it shows the
7 second highest correlation coefficient for OP. The link to biomass-burning seems to be generally
8 weak at this altitude and topographical location in the cordillera.

9 The situation changes for the *El Tiro* up-valley MS, where the highest correlations occur between
10 rain concentrations and anthropogenic sources and between OP concentrations and biomass-
11 burning sources.

12 Even if the correlation coefficients are low, they show interesting tendencies. For *El Tiro* site,
13 volcanic and anthropogenic emissions are more clearly related to rain concentrations while the
14 opposite is true for biomass-burning, which is more strongly related to OP concentrations. OMI
15 shows a mixed behavior because it includes volcanic as well as regional anthropogenic emissions
16 as shown in Tab. 2 and Fig. 4.

17 Rather low correlation coefficients mean that no unique source can totally explain the oscillations
18 in the concentrations. Furthermore, correlation coefficients are blurred because peaks are extreme
19 values, which represent scatter. The concentration time-series are a sum curve of all transport
20 values. By exploring time-series of sink and transport from sources, the next subsection (4.2.2)
21 sheds some light on what groups of transport variables explain the most of the variability in the
22 concentration variables.

23 **4.2.2 Analysis of monthly time-series**

24 Figure 5 shows the time series of SO₂ transport (concentrations at the pixels above the study site)
25 and the respective sulfate concentrations observed at the sites. We observed that mainly
26 depending on emission state and air mass history, emission peaks resulted in concentration peaks
27 of different intensity. One general finding is that the peak concentrations in biomass-burning
28 transport were ~56 times higher than those of the other sources. Besides this there was a slight
29 tendency for increasing emissions from anthropogenic, regional and even volcanic sources in the

1 observation period. At the same time, emissions due to biomass-burning decreased, particularly
2 in the last years of the study period (2008, 2009) which is consistent with deforestation statistics
3 in Brazil (Hansen et al., 2013; Rodrigues-Ramos et al., 2011; Torres et al., 2010).

4 Regarding relations between wind direction and the link between sources and sinks it is obvious
5 that during easterly airstreams coinciding with the Amazon biomass-burning season from August
6 to October (dark grey bars) (Andreae et al., 2004), biomass emission peaks caused concentration
7 peaks. Contrary to this, during wind conditions from the northern and western sector (light grey),
8 peaks in volcanic activity and anthropogenic emissions in central/northern Ecuador could be
9 clearly related to concentration peaks.

10 *El Tiro* MS had higher sulfate loads in fog than in rain. A decrease following the reduction in
11 biomass-burning was observed in the OP sulfate concentration time-series from 2007 to 2008
12 with a violent upturn at the end of the biomass-burning season of 2009 (Fig. 5a) for which we
13 have not found any explanation yet; this last peak is responsible for the light positive tendency of
14 the curve. Rain sulfate time-series (Fig. 5b) presented a small negative tendency over the
15 observed period (2005-2009).

16 In OP, only one peak in the biomass-burning time-series (July 2008) seemed to dominate the
17 resulting concentrations. Volcanic transport did not play a role. In rain, biomass-burning and
18 volcanic transport peaks were both reflected in the concentration time series, with a stronger
19 coincidence with volcanic emissions. Anthropogenic sources and rain water sulfate
20 concentrations showed the same peak coincidences at *El Tiro* during northerly winds (particularly
21 in 2005 and 2008). However, volcanic transport was quantitatively higher than that from
22 anthropogenic sources, which means that it likely contributes more to the deposition.

23 At the uppermost and more exposed *Cerro del Consuelo* MS we observe a different situation,
24 namely a very small negative tendency in the sulfate concentrations in both OP (Fig. 5a) and rain
25 (Fig. 5b). OP sulfate concentrations are also higher than in rain here. In this case, the negative
26 trend of the biomass-burning SO₂ transport with the highest transport (Fig. 5e) seems to dominate
27 the concentration's temporal development irrespective of the type of precipitation. Biomass-
28 burning peaks are affecting only rain concentrations, except for one emission peak in August
29 2005, which is affecting both OP and rain concentrations (this is more or less the same for *El*
30 *Tiro* MS). Interestingly, volcanic transport peaks (Fig. 5d) are mostly affecting OP
31 concentrations. This is definitely different from *El Tiro* MS, where no influence in OP

1 concentrations was noticed. EDGAR anthropogenic transport (Fig. 5f) is nonetheless also
2 reflected in OP concentrations, but again here the transport was quantitatively lower.

3 Between March and May 2005-2007 a small peak in the biomass-burning SO₂ transport time-
4 series can be seen, which very likely corresponds to the emissions of the Venezuelan savanna's
5 biomass-burning season as observed by Hamburger et al. (2013). Apparently, this biomass-
6 burning emission source has no significant resonance in the deposition at our study site. In 2008
7 and 2009 the peaks almost disappear, again coinciding with the anomalous biomass-burning
8 season these two years (Torres et al., 2010).

9 4.2.3 Factor analysis

10 Table 4 presents the results from factor analysis applied to observational and modeled data. A
11 main outcome is that the three first factors explain more than 80% of the variance for both *El*
12 *Tiro* and *Cerro del Consuelo* MSs.

13 For *Cerro del Consuelo* MS, the eigenvectors show that biomass-burning SO₂ transport (GFED)
14 was related to the sulfate concentrations in rain, since both loaded to the factors 2 and 3. The rest
15 was more closely related to sulfate concentrations in OP, with loadings to factors 1, 4 and 5. The
16 communalities also show that factor 2 was dominated by biomass-burning SO₂ (GFED) and rain
17 sulfate concentrations. Factor 1 shows important loadings of OP sulfate concentrations and SO₂
18 transport from all other source datasets (OMI, Aerocom, and EDGAR).

19 At *El Tiro* MS, the relationship was inverse; biomass-burning SO₂ modeled transport and OP SO₂
20 concentrations were more closely related, both of them contributing to factor 2. Loadings from
21 rain sulfate concentrations and all other source dataset contributed to factor 1, and therefore they
22 lied close in the multidimensional space. This is stressed by the communalities, where both the
23 variance of OP sulfate concentrations and biomass-burning SO₂ transport contributed mainly to
24 factor 2, and rain sulfate concentrations and the SO₂ transport from the rest of emission sources to
25 factor 1.

26

27 5 Discussion

28 In this study, we concerned ourselves with the identification of important natural and

1 anthropogenic sources contributing to atmospheric sulfate deposition in the tropical mountain
2 forests of south-eastern Ecuador. Special attention was given to the contribution of natural
3 volcanic emissions, given that the study site is located in a region with a very high density of
4 active volcanoes (Carn et al., 2008).

5 Based on fire pixels, emission inventories, and back-trajectories several previous studies (Fabian
6 et al., 2005, 2009; Rollenbeck, 2010; Rollenbeck et al., 2006) pin pointed biomass-burning as the
7 principal source of atmospheric sulfate. These did not use, however, neither data on explosive
8 emissions nor passive degassing, which represents a considerable part of the total volcanic
9 emissions (Carn et al., 2008). Because of the latter argument, we came to the idea that the
10 contribution of volcanoes to the sulfate deposition in the area could have being underestimated.

11 Contrary to what we expected, we found that, quantitatively, volcanic emission sources did not
12 play a substantial role, even if they were more important than anthropogenic emissions. Biomass-
13 burning sources were indeed dominant substantially for two reasons: first, because easterlies are
14 strong and constant, which is translated in preponderant air-mass-transport from the east (Bendix
15 et al., 2008b), where the main biomass-burning region is located; second, because biomass-
16 burning emissions in the Brazilian Amazon are strong and the area burned covers a very large
17 surface (Giglio et al., 2010; Prins and Menzel, 1992), making it more likely for the emissions to
18 be advected. Transport from the north and west occurred only for short periods and the sources of
19 SO₂ did not cover such a big surface as biomass-burning in the Brazilian Amazon did (Fig. 4c).
20 However, no single emission sources explained the variability in the deposition but a sum of
21 single contributions, always depending on the type of precipitation and the topographic features
22 of the site where samples were gathered.

23 The correlation analysis between SO₂ transport and sulfate concentrations resulted in some
24 significant but not so strong correlations. Furthermore, the comparison of time-series revealed
25 that no single transport curve completely matches neither OP nor rain concentrations. The
26 different source-related transport curves coincided only in specific time-periods with the
27 concentration curves, producing OP and/or rain deposition depending on the location of the MS.
28 This is clarified in the following subsections and a graphical interpretation is given in Fig. 6.

29 **5.1 Easterly transport**

30 The correlation between *El Tiro* MS and biomass-burning transport was significant but weak

1 only for OP samples. This relationship was supported by factor analysis.

2 In the period from August to October, the tropical easterlies still blow strongly and persistently
3 and overlap with the occurrence of the biomass-burning season in the Amazon basin. Sulfur
4 emissions, basically from the Brazilian Amazon, are transported towards the west until they
5 encounter the first foothills and cordilleras of the Andean mountain range, where intense
6 scavenging of pollutants takes place. The connection to the emissions in the Amazon basin is
7 mainly noticed in OP sulfate concentrations from *El Tiro* MS (dark grey bars in Fig. 5a, e). Here
8 concentration peaks coincide with SO₂ transport. Biomass-burning has a mean low injection
9 height into the atmosphere (max. 3 km, but only a very thin haze, while the main heating at 850
10 hPa represents a mean injection height of 1.5 km, Davidi et al., 2009) which means that the
11 pollution is transported in the lower valley upwards with the upvalley winds and hit the fog
12 collectors at *El Tiro* (2660 m.a.s.l.).

13 The same easterly air-masses hit the mountain on which top *Cerro del Consuelo* MS is located,
14 and are adiabatically uplifted producing intense rainfall and OP mainly windward but also on the
15 summit. The fog collector is not located directly on the windward hillside, exposed to ascending
16 airmasses, so the ion loaded water is apparently mostly collected by the rain gauges, as shown by
17 time-series and factor analysis. However, measurements from fog collectors and rain gauges
18 overlap here more frequently than at *El Tiro*, making the separation between rain and OP more
19 difficult. The result is that rain and OP differentiation is fuzzy, which is blurring the correlations
20 between concentrations and transport. Hence, the biomass-burning signal is relatively low here.

21 **5.2 Northerly and westerly transport**

22 Volcanic and anthropogenic transport were significantly correlated to sulfate concentrations from
23 *El Tiro* MS rain samples and OP samples from *Cerro del Consuelo* MS. The same was also
24 reflected in the results of the factor analysis.

25 Between October and January, as northerlies set in, the volcanic SO₂ transport time-series
26 coincide with those of sulfate concentrations from the MSs, especially regarding sulfate in rain,
27 from *El Tiro* MS, and in OP from *Cerro del Consuelo* MS. The greater recurrence of
28 coincidences with the rain time-series at *El Tiro* MS is explained by its location at a mountain
29 pass which links the eastern slopes and the interandean valley of Loja. The two parallel east-to-
30 west mountain ranges mark the boundaries of the San Francisco Valley. As already mentioned

1 (section 5.1), they shape the wind field, favoring the advected polluted air-masses coming from
2 the east or west, like biomass-burning transport, to impact the vegetation and the east-west
3 oriented fog collectors on the mountain pass. Clouds advected from the north and north-west
4 (likely charged with SO₂ ions) are partially blocked by the delimiting mountain range at the
5 north. Hence, only rain gauges can collect sulfate scavenged from these clouds as rain drops
6 traverse the atmosphere on their way to the ground.

7 Between 20% and 50% of wind trajectories reach the RBSF from the north, overpassing areas of
8 active volcanoes. Volcanoes in the Andes lie at altitudes that in most of the cases exceed the 4000
9 m.a.s.l., so even emissions from degassing can contaminate high clouds in the lower troposphere
10 (Diehl et al., 2012; Stuefer et al., 2012). These months there is also an increment in the transport
11 of anthropogenic SO₂, most likely in response to the air masses passing over emission sources
12 from Ecuadorian and maybe Colombian cities. Anthropogenic sources in the Andes north of the
13 RBSF also lie at high altitudes and, as recent studies reported for Europe, this type of emissions
14 can also reach higher atmospheric levels as previously assumed (Bieser et al., 2011). The latter
15 would make anthropogenic plumes from Ecuadorian big cities in the Andes prone to reach higher
16 clouds in the atmosphere as well. Therefore, northerly air-masses charged with volcanic sulfate
17 particles, and to a lesser extent anthropogenic, directly impinges the mountain where *Cerro del*
18 *Consuelo* fog collector is located on the windward (north facing slopes) side. OP water is here a
19 major part of precipitation (41% of rainfall; Bendix et al., 2008). In addition, it is located at 3200
20 m.a.s.l., probably more exposed to pollutants transported through higher atmospheric levels than
21 at *El Tiro* MS. Multicollinearity found between volcanic, anthropogenic, and regional
22 (Ecuadorian) transport datasets reinforces this hypothesis (Tab. 2).

23

24 **6 Conclusions**

25 We conclude that biomass-burning sources are dominating the sulfate deposition as a result of
26 strong and persistent easterly sulfate transport of emissions from wide burned areas of Amazon
27 forests and its anthropogenic replacement systems. These take place during the main Amazon
28 biomass-burning season between August and October. Between October and December, the main
29 wind direction shifts to the north and west, transporting volcanic and anthropogenic sulfate to our
30 study site. The transport from these sources is, nonetheless, much inferior compared to biomass-

1 burning.

2 We found two different deposition regimes at the evaluated topographic sites. The up-valley
3 mountain pass *El Tiro*, is located on the eastern side of the ridge and is characterized by a more
4 advective environment with dominating OP deposition from low tropospheric fire-polluted air-
5 masses from the Amazon lowlands. Sulfate from volcanic and anthropogenic emissions are
6 episodically transported through a higher atmospheric level from the north and, as there is no
7 cloud immersion during this wind directions, sulfate can be only deposited by rain.

8 At the highest mountain crest of the study area, *Cerro del Consuelo*, the situation is less
9 homogeneous and less clear. Deposition was dominated by OP until 2007, when it started to be
10 dominated by rain. Sulfate deposition by OP is likely linked to volcanic and anthropogenic
11 sources in the north, as a consequence of its higher location and its orientation. The higher
12 atmospheric transport reaches *Cerro del Consuelo* MS from all wind directions and thus
13 contaminate the cloud fog resulting in OP deposition. According to the cross-correlation results,
14 biomass-burning has no significant relation to this site's deposition. Overlapping of rain gauge
15 and fog collector measurements made the differentiation of deposition types difficult. However,
16 time-series and factor analyses show a likely contribution of human induced fires in the lowlands
17 to sulfate deposition by rain at *Cerro del Consuelo* MS. The higher conductivity of the rain
18 samples point to the likely higher contamination of the rain samples as well.

19 In general, this study revealed that even if volcanic emission are proximate and numerous, they
20 do not dominate the sulfate deposition at the RBSF. The shape and size of the sources, as well as
21 the consistency of the winds are important parameters that determined the dominance of biomass-
22 burning in the deposition at the study site. However, the importance of topography has also been
23 stressed as important parameter conditioning the type and quantity of deposition in areas with
24 complex terrain.

25

26 **Author contribution**

27 J. B., R. R., and S.M.G. designed the experiments and S. M. G. carried them out. R. R.
28 developed the trajectory model code and S. M. G. performed the simulations. S. M. G. and K.T.
29 collected, processed, and adapted the satellite data and emission inventories to the format
30 requested for model runs. S. M. G. analyzed the data and prepared the manuscript with

1 contributions from all co-authors.

2

3 **Acknowledgements**

4 We thank the German Academic Exchange Service (DAAD) for funding the PhD thesis of
5 Sandro Makowski Giannoni (Ref. Number A/08/98222) and the German Research Foundation
6 (DFG) for the funding of the work in the scope of the Research Unit RU816 (funding number:
7 BE 1780/15-1). We are grateful to Lukas Lehnert, Nicolas Caspari, and Maik Dobermann for
8 their valuable help. We also thank the foundation Nature & Culture International (NCI) Loja and
9 San Diego for logistic support. We finally thank Giulia F. Curatola Fernández for proof reading.

10

11 **References**

12 Andreae, M. O., Rosenfeld, D., Artaxo, P., Costa, A. A., Frank, G. P., Longo, K. M. and Silva-
13 Dias, M. A. F.: Smoking rain clouds over the Amazon, *Science*, 303(5662), 1337–42,
14 doi:10.1126/science.1092779, 2004.

15 Beck, E., Bendix, J., Kottke, I., Makeschin, F. and Mosandl, R., Eds.: Gradients in a tropical
16 mountain ecosystem of Ecuador, Springer Berlin / Heidelberg, Berlin, Germany., 2008.

17 Beiderwieden, E., Wrzesinsky, T. and Klemm, O.: Chemical characterization of fog and rain
18 water collected at the eastern Andes cordillera, *Hydrol. Earth Syst. Sci.*, 9(3), 185–191,
19 doi:10.5194/hess-9-185-2005, 2005.

20 Bendix, J. and Beck, E.: Spatial aspects of ecosystem research in a biodiversity hot spot of
21 southern Ecuador – an introduction, *Erdkunde*, 63(4), 305–308,
22 doi:10.3112/erdkunde.2009.04.01, 2009.

23 Bendix, J., Beck, E., Bräuning, A., Makeschin, F., Mosandl, R., Scheu, S. and Wilcke, W., Eds.:
24 Ecosystem Services, Biodiversity and Environmental Change in a Tropical Mountain Ecosystem
25 of South Ecuador, Springer Berlin/Heidelberg, Berlin, Germany., 2013.

26 Bendix, J., Rollenbeck, R., Göttlicher, D. and Cermak, J.: Cloud occurrence and cloud properties
27 in Ecuador, *Clim. Res.*, 30, 133–147, doi:10.3354/cr030133, 2006a.

1 Bendix, J., Rollenbeck, R., Göttlischer, D., Nauß, T. and Fabian, P.: Seasonality and diurnal
2 pattern of very low clouds in a deeply incised valley of the eastern tropical Andes (South
3 Ecuador) as observed by a cost-effective WebCam system, *Meteorol. Appl.*, 15, 281–291,
4 doi:10.1002/met, 2008a.

5 Bendix, J., Rollenbeck, R. and Reudenbach, C.: Diurnal patterns of rainfall in a tropical Andean
6 valley of southern Ecuador as seen by a vertically pointing K-band Doppler radar, *Int. J.*
7 *Climatol.*, 26, 829–846, doi:10.1002/joc.1267, 2006b.

8 Bendix, J., Rollenbeck, R., Richter, M., Fabian, P. and Emck, P.: Climate, in *Gradients in a*
9 *Tropical Mountain Ecosystem of Ecuador*, edited by E. Beck, J. Bendix, I. Kottke, F. Makeschin,
10 and R. Mosandl, pp. 63–74, Springer Berlin / Heidelberg. [online] Available from:
11 http://dx.doi.org/10.1007/978-3-540-73526-7_8, 2008b.

12 Bieser, J., Aulinger, A., Matthias, V., Quante, M. and Denier van der Gon, H. a C.: Vertical
13 emission profiles for Europe based on plume rise calculations, *Environ. Pollut.*, 159(10), 2935–
14 2946, doi:10.1016/j.envpol.2011.04.030, 2011.

15 Boy, J., Rollenbeck, R., Valarezo, C. and Wilcke, W.: Amazonian biomass burning-derived acid
16 and nutrient deposition in the north Andean montane forest of Ecuador, *Global Biogeochem.*
17 *Cycles*, 22, GB4011 [online] Available from: <http://dx.doi.org/10.1029/2007GB003158>, 2008.

18 Carn, S. A., Krotkov, N. A., Yang, K., Hoff, R. M., Prata, A. J., Krueger, A. J., Loughlin, S. C.
19 and Levelt, P. F.: Extended observations of volcanic SO₂ and sulfate aerosol in the stratosphere,
20 *Atmos. Chem. Phys. Discuss.*, 7, 2857–2871, doi:10.5194/acpd-7-2857-2007, 2007.

21 Carn, S. A., Krueger, A. J., Arellano, S., Krotkov, N. A. and Yang, K.: Daily monitoring of
22 Ecuadorian volcanic degassing from space, *J. Volcanol. Geotherm. Res.*, 176, 141–150, doi:DOI:
23 10.1016/j.jvolgeores.2008.01.029, 2008.

24 Crutzen, P. J. and Andreae, M. O.: Biomass burning in the tropics: impact on atmospheric
25 chemistry and biogeochemical cycles, *Science*, 250, 1669–1678,
26 doi:10.1126/science.250.4988.1669, 1990.

27 Curatola Fernández, G. F., Silva, B., Gawlik, J., Thies, B. and Bendix, J.: Bracken fern frond
28 status classification in the Andes of southern Ecuador: combining multispectral satellite data and
29 field spectroscopy, *Int. J. Remote Sens.*, 34(20), 7020–7037,

1 doi:10.1080/01431161.2013.813091, 2013.

2 Davidi, A., Koren, I. and Remer, L.: Direct measurements of the effect of biomass burning over
3 the Amazon on the atmospheric temperature profile, *Atmos. Chem. Phys.*, 9(21), 8211–8221,
4 doi:10.5194/acp-9-8211-2009, 2009.

5 Delmelle, P., Stix, J., Baxter, P. J. and B, G.-A. J.: Atmospheric dispersion, environmental effects
6 and potential health hazard associated with the low-altitude gas plume of Masaya volcano,
7 Nicaragua, *Bull. Volcanol.*, 64(6), 423–434, doi:10.1007/s00445-002-0221-6, 2002.

8 Delmelle, P., Stix, J., Bourque, C. P.-A., Baxter, P. J., Garcia-Alvarez, J. and Barquero, J.: Dry
9 Deposition and Heavy Acid Loading in the Vicinity of Masaya Volcano, a Major Sulfur and
10 Chlorine Source in Nicaragua, *Environ. Sci. Technol.*, 35(7), 1289–1293,
11 doi:10.1021/es000153m, 2001.

12 Dentener, F., Drevet, J., Lamarque, J. F., Bey, I., Eickhout, B., Fiore, A. M., Hauglustaine, D.,
13 Horowitz, L. W., Krol, M., Kulshrestha, U. C., Lawrence, M., Galy-Lacaux, C., Rast, S.,
14 Shindell, D., Stevenson, D., Van Noije, T., Atherton, C., Bell, N., Bergman, D., Butler, T.,
15 Cofala, J., Collins, B., Doherty, R., Ellingsen, K., Galloway, J., Gauss, M., Montanaro, V.,
16 Müller, J. F., Pitari, G., Rodriguez, J., Sanderson, M., Solmon, F., Strahan, S., Schultz, M., Sudo,
17 K., Szopa, S. and Wild, O.: Nitrogen and sulfur deposition on regional and global scales: A
18 multimodel evaluation, *Global Biogeochem. Cycles*, 20(4), GB4003,
19 doi:10.1029/2005GB002672, 2006.

20 Diehl, T., Heil, A., Chin, M., Pan, X., Streets, D., Schultz, M. and Kinne, S.: Anthropogenic,
21 biomass burning, and volcanic emissions of black carbon, organic carbon, and SO₂ from 1980 to
22 2010 for hindcast model experiments, *Atmos. Chem. Phys. Discuss.*, 12(9), 24895–24954,
23 doi:10.5194/acpd-12-24895-2012, 2012.

24 Eklund, T., McDowell, W. and Pringle, C.: Seasonal variation of tropical precipitation chemistry:
25 La Selva, Costa Rica, *Atmos. Environ.*, 31(23), 3903–3910 [online] Available from:
26 <http://www.sciencedirect.com/science/article/pii/S135223109700246X> (Accessed 20 February
27 2014), 1997.

28 Elser, J. J., Bracken, M. E. S., Cleland, E. E., Gruner, D. S., Harpole, W. S., Hillebrand, H., Ngai,
29 J. T., Seabloom, E. W., Shurin, J. B. and Smith, J. E.: Global analysis of nitrogen and phosphorus
30 limitation of primary producers in freshwater, marine and terrestrial ecosystems, *Ecol. Lett.*,

1 10(12), 1135–42, doi:10.1111/j.1461-0248.2007.01113.x, 2007.

2 Emck, P.: A climatology of South Ecuador, University of Erlangen. [online] Available from:
3 <http://www.opus.ub.uni-erlangen.de/opus/volltexte/2007/656/> (Accessed 15 August 2012), 2007.

4 Fabian, P., Kohlpaintner, M. and Rollenbeck, R.: Biomass burning in the Amazon-fertilizer for
5 the mountaineous rain forest in Ecuador, *Environ. Sci. Pollut. Res.*, 12(5), 290–296 [online]
6 Available from: <http://dx.doi.org/10.1065/espr2005.07.272>, 2005.

7 Fabian, P., Rollenbeck, R., Spichtinger, N., Brothers, L., Dominguez, G. and Thiemens, M.:
8 Sahara dust, ocean spray, volcanoes, biomass burning: pathways of nutrients into Andean
9 rainforests, *Adv. Geosci.*, 22, 85–94, 2009.

10 Giglio, L., Randerson, J. T., van der Werf, G. R., Kasibhatla, P. S., Collatz, G. J., Morton, D. C.
11 and DeFries, R. S.: Assessing variability and long-term trends in burned area by merging
12 multiple satellite fire products, *Biogeosciences*, 7(3), 1171–1186, doi:10.5194/bg-7-1171-2010,
13 2010.

14 Gordon, C., Herrera, R. and Hutchinson, T.: Studies of fog events at two cloud forests near
15 Caracas, Venezuela—II. Chemistry of fog, *Atmos. Environ.*, 28(2), 323–337 [online] Available
16 from: <http://www.sciencedirect.com/science/article/pii/1352231094901082> (Accessed 23 May
17 2012), 1994.

18 Graf, H.-F., Feichter, J. and Langmann, B.: Volcanic sulfur emissions: Estimates of source
19 strength and its contribution to the global sulfate distribution, *J. Geophys. Res.*, 102(D9), 10727,
20 doi:10.1029/96JD03265, 1997.

21 Greaver, T. L., Sullivan, T. J., Herrick, J. D., Barber, M. C., Baron, J. S., Cosby, B. J., Deerhake,
22 M. E., Dennis, R. L., Dubois, J.-J. B., Goodale, C. L., Herlihy, A. T., Lawrence, G. B., Liu, L.,
23 Lynch, J. A. and Novak, K. J.: Ecological effects of nitrogen and sulfur air pollution in the US:
24 what do we know?, *Front. Ecol. Environ.*, 10(7), 365–372, doi:10.1890/110049, 2012.

25 Hamburger, T., Matisāns, M., Tunved, P., Ström, J., Calderon, S., Hoffmann, P., Hochschild, G.,
26 Gross, J., Schmeissner, T., Wiedensohler, A. and Krejci, R.: Long-term in situ observations of
27 biomass burning aerosol at a high altitude station in Venezuela – sources, impacts and interannual
28 variability, *Atmos. Chem. Phys.*, 13(19), 9837–9853, doi:10.5194/acp-13-9837-2013, 2013.

29 Hansen, J., Ruedy, R., Sato, M. and Lo, K.: Global surface temperature change, *Rev. Geophys.*,

1 48, RG4004, doi:10.1029/2010RG000345, 2010.

2 Hansen, M. C., Potapov, P. V, Moore, R., Hancher, M., Turubanova, S. A., Tyukavina, A., Thau,
3 D., Stehman, S. V, Goetz, S. J., Loveland, T. R., Kommareddy, A., Egorov, A., Chini, L., Justice,
4 C. O. and Townshend, J. R. G.: High-resolution global maps of 21st-century forest cover change,
5 Science, 342(6160), 850–853, doi:10.1126/science.1244693, 2013.

6 Hartig, K. and Beck, E.: The bracken fern (*Pteridium arachnoideum* (Kaulf.) Maxon) dilemma in
7 the Andes of Southern Ecuador, *Ecotropica*, 9, 3–13, 2003.

8 (INEC), I. N. de E. y C.: Fascículo provincial Zamora Chinchipe, Result. del censo población y
9 vivienda [online] Available from: [http://www.ecuadorencifras.gob.ec/wp-](http://www.ecuadorencifras.gob.ec/wp-content/descargas/Manu-lateral/Resultados-provinciales/)
10 [content/descargas/Manu-lateral/Resultados-provinciales/](http://www.ecuadorencifras.gob.ec/wp-content/descargas/Manu-lateral/Resultados-provinciales/), 2010.

11 Janssens-Maenhout, G., Dentener, F., Aardenne, J. van, Monni, S., Pagliari, V., Orlandini, L.,
12 Klimont, Z., Kurokawa, J., Akimoto, H., Ohara, T., Wankmüller, R., Battye, B., Grano, D.,
13 Zuber, A. and Keating, T.: EDGAR-HTAP: a harmonized gridded air pollution emission dataset
14 based on national inventories, Ispra, Italy., 2012.

15 Kuylenstierna, J. C. I., Rodhe, H., Cinderby, S. and Hicks, K.: Acidification in developing
16 countries: ecosystem sensitivity and the critical load approach on a global scale, *AMBIO A J.*
17 *Hum. Environ.*, 30(1), 20–28, doi:10.1579/0044-7447-30.1.20, 2001.

18 Langmann, B. and Graf, H. F.: Indonesian smoke aerosols from peat fires and the contribution
19 from volcanic sulfur emissions, *Geophys. Res. Lett.*, 30(11), 1547, doi:10.1029/2002GL016646,
20 2003.

21 Lee, C., Martin, R. V, van Donkelaar, A., Lee, H., Dickerson, R. R., Hains, J. C., Krotkov, N.,
22 Richter, A., Vinnikov, K. and Schwab, J. J.: SO₂ emissions and lifetimes: estimates from inverse
23 modeling using in situ and global, space-based (SCIAMACHY and OMI) observations, *J.*
24 *Geophys. Res.*, 116(D6), D06304 [online] Available from:
25 <http://dx.doi.org/10.1029/2010JD014758>, 2011.

26 Ljung, K., Maley, F., Cook, A. and Weinstein, P.: Acid sulfate soils and human health—A
27 Millennium Ecosystem Assessment, *Environ. Int.*, 35(8), 1234–1242,
28 doi:10.1016/j.envint.2009.07.002, 2009.

29 Makowski Giannoni, S., Rollenbeck, R., Fabian, P. and Bendix, J.: Complex topography

1 influences atmospheric nitrate deposition in a neotropical mountain rainforest, *Atmos. Environ.*,
2 79, 385–394, doi:10.1016/j.atmosenv.2013.06.023, 2013.

3 Menz, F. C. and Seip, H. M.: Acid rain in Europe and the United States: an update, *Environ. Sci.*
4 *Policy*, 7(4), 253–265, doi:10.1016/j.envsci.2004.05.005, 2004.

5 Morales, J., Bifano, C. and Escalona, A.: Atmospheric deposition of SO₄-S and (NH₄⁺ NO₃)-N
6 at two rural sites in the Western Maracaibo Lake Basin, Venezuela, *Atmos. Environ.*, 32(17),
7 3051–3058 [online] Available from:
8 <http://www.sciencedirect.com/science/article/pii/S135223109700160X> (Accessed 21 August
9 2012), 1998.

10 Mu, M., Randerson, J. T., Van der Werf, G. R., Giglio, L., Kasibhatla, P., Morton, D., Collatz, G.
11 J., DeFries, R. S., Hyer, E. J., PRINS, E. M., Griffith, D. W. T., Wunch, D., Toon, G. C.,
12 Sherlock, V. and Wennberg, P. O.: Daily and 3-hourly variability in global fire emissions and
13 consequences for atmospheric model predictions of carbon monoxide, *J. Geophys. Res.*,
14 116(D24), D24303 [online] Available from:
15 <http://www.agu.org/journals/jd/jd1124/2011JD016245/2011jd016245-t04.txt> (Accessed 23
16 January 2014), 2011.

17 Pauliquevis, T., Lara, L. L., Antunes, M. L. and Artaxo, P.: Aerosol and precipitation chemistry
18 measurements in a remote site in Central Amazonia: the role of biogenic contribution, *Atmos.*
19 *Chem. Phys.*, 12(11), 4987–5015, doi:10.5194/acp-12-4987-2012, 2012.

20 Pfeffer, M. a., Langmann, B. and Graf, H.-F.: Atmospheric transport and deposition of
21 Indonesian volcanic emissions, *Atmos. Chem. Phys.*, 6(9), 2525–2537, doi:10.5194/acp-6-2525-
22 2006, 2006.

23 Phoenix, G. K., Hicks, K. W., Cinderby, S., Kuylenstierna, J. C. I., Stock, W. D., Dentener, F. J.,
24 Giller, K. E., Austin, A. T., Lefroy, R. D. B., Gimeno, B. S., Ashmore, M. R. and Ineson, P.:
25 Atmospheric nitrogen deposition in world biodiversity hotspots: The need for a greater global
26 perspective in assessing N deposition impacts, *Glob. Chang. Biol.*, 12(3), 470–476,
27 doi:10.1111/j.1365-2486.2006.01104.x, 2006.

28 Prins, E. M. and Menzel, W. P.: Geostationary satellite detection of biomass burning in South
29 America, *Int. J. Remote Sens.*, 13(15), 2783–2799, doi:10.1080/01431169208904081, 1992.

30 Rissler, J., Vestin, A., Swietlicki, E., Fisch, G., Zhou, J., Artaxo, P. and Andreae, M. O.: Size

1 distribution and hygroscopic properties of aerosol particles from dry-season biomass burning in
2 Amazonia, *Atmos. Chem. Phys.*, 6(2), 471–491, doi:10.5194/acp-6-471-2006, 2006.

3 Rodrigues-Ramos, A., Prado do Nascimento, E. and Oliveira, M.: Temporada de incêndios
4 florestais no Brasil em 2010: análise de série histórica de 2005 a 2010 e as influências das chuvas
5 e do desmatamento na quantidade dos focos de calor, in *Simpósio Brasileiro de Sensoriamento*
6 *Remoto*, pp. 7902–7909, Curitiba. [online] Available from:
7 <http://www.dsr.inpe.br/sbsr2011/files/p1414.pdf> (Accessed 19 February 2014), 2011.

8 Rollenbeck, R.: Global sources-local impacts: natural and anthropogenic sources of matter
9 deposition in the Andes of Ecuador, *Geo-öko*, (31), 5–27, 2010.

10 Rollenbeck, R., Bendix, J. and Fabian, P.: Spatial and temporal dynamics of atmospheric water
11 inputs in tropical mountain forests of South Ecuador, *Hydrol. Process.*, 25(3), 344–352,
12 doi:10.1002/hyp.7799, 2011.

13 Rollenbeck, R., Bendix, J., Fabian, P., Boy, J., Wilcke, W., Dalitz, H., Oesker, M. and Emck, P.:
14 Comparison of different techniques for the measurement of precipitation in tropical montane rain
15 forest regions, *J. Atmos. Ocean. Technol.*, 24(2), 156–168, doi:10.1175/JTECH1970.1, 2007.

16 Rollenbeck, R., Fabian, P. and Bendix, J.: Precipitation dynamics and chemical properties in
17 tropical mountain forests of Ecuador, *Adv. Geosci.*, 6, 73–76 [online] Available from:
18 <http://hal.archives-ouvertes.fr/hal-00296900/> (Accessed 10 February 2014), 2006.

19 Rudel, T. K., Coomes, O. T., Moran, E., Achard, F., Angelsen, A., Xu, J. and Lambin, E.: Forest
20 transitions: towards a global understanding of land use change, *Glob. Environ. Chang.*, 15(1),
21 23–31, doi:10.1016/j.gloenvcha.2004.11.001, 2005.

22 Schemenauer, R., Banic, C. and Urquizo, N.: High elevation fog and precipitation chemistry in
23 southern Quebec, Canada, *Atmos. Environ.*, 29(17), 2235–2252 [online] Available from:
24 <http://www.sciencedirect.com/science/article/pii/S135223109500153P> (Accessed 26 August
25 2014), 1995.

26 Schemenauer, R. S. and Cereceda, P.: A proposed standard fog collector for use in high-elevation
27 regions, *J. Appl. Meteorol.*, 33, 1313–1322 [online] Available from:
28 <http://adsabs.harvard.edu/abs/1994JApMe..33.1313S> (Accessed 22 November 2011), 1994.

29 Sigha-Nkamdjou, L., Galy-Lacaux, C., Pont, V., Richard, S., Sighomnou, D. and Lacaux, J.:

1 Rainwater chemistry and wet deposition over the equatorial forested ecosystem of Zoétélé
2 (Cameroon), *J. Atmos. Chem.*, 46, 173–198 [online] Available from:
3 <http://link.springer.com/article/10.1023/A:1026057413640> (Accessed 20 February 2014), 2003.

4 Smith, S. J., van Aardenne, J., Klimont, Z., Andres, R. J., Volke, A. and Delgado Arias, S.:
5 Anthropogenic sulfur dioxide emissions: 1850–2005, *Atmos. Chem. Phys.*, 11(3), 1101–1116,
6 doi:10.5194/acp-11-1101-2011, 2011.

7 Stevenson, D. S., Johnson, C. E., Collins, W. J. and Derwent, R. G.: The tropospheric sulphur
8 cycle and the role of volcanic SO₂, *Geol. Soc. London, Spec. Publ.*, 213(1), 295–305,
9 doi:10.1144/GSL.SP.2003.213.01.18, 2003.

10 Stuefer, M., Freitas, S. R., Grell, G., Webley, P., Peckham, S. and McKeen, S. A.: Inclusion of
11 Ash and SO₂ emissions from volcanic eruptions in WRF-CHEM: development and some
12 applications, *Geosci. Model Dev. Discuss.*, 5(3), 2571–2597, doi:10.5194/gmdd-5-2571-2012,
13 2012.

14 Torres, O., Chen, Z., Jethva, H., Ahn, C., Freitas, S. R. and Bhartia, P. K.: OMI and MODIS
15 observations of the anomalous 2008–2009 Southern Hemisphere biomass burning seasons,
16 *Atmos. Chem. Phys.*, 10(8), 3505–3513, doi:10.5194/acp-10-3505-2010, 2010.

17 Van der Werf, G. R., Randerson, J. T., Giglio, L., Collatz, G. J., Mu, M., Kasibhatla, P. S.,
18 Morton, D. C., DeFries, R. S., Jin, Y. and van Leeuwen, T. T.: Global fire emissions and the
19 contribution of deforestation, savanna, forest, agricultural, and peat fires (1997–2009), *Atmos.*
20 *Chem. Phys.*, 10(23), 11707–11735, doi:10.5194/acp-10-11707-2010, 2010.

21 Wullaert, H., Homeier, J., Valarezo, C. and Wilcke, W.: Response of the N and P cycles of an
22 old-growth montane forest in Ecuador to experimental low-level N and P amendments, *For. Ecol.*
23 *Manage.*, 260(9), 1434–1445, doi:10.1016/j.foreco.2010.07.021, 2010.

1 Table 1: pH and conductivity summary statistics in Occult Precipitation (OP) and rain samples
 2 from *El Tiro* and *Cerro del Consuelo* Meteorological Stations (MSs).

	<i>El Tiro</i>		<i>Cerro del Consuelo</i>	
	OP	Rain	OP	Rain
Median pH	4.8 MAD= 0.37	5.4 MAD= 0.51	5 MAD=0.29	5.3 Mad=0.36
Min-max pH	2.4-5.8	3.7-6.7	1.8-6.2	3-6.1
Median conductivity (S/m)	10.9 MAD=6.4	3.7 MAD=1.6	2.6 MAD=1	8.1 MAD=6.8
Min-max conductivity (S/m)	2.3-110.3	1.4-45.4	1.4-12.4	1.7-72

1 Table 2: Cross-correlation of calculated SO₂ concentration time-series over *El Tiro* and *Cerro del*
 2 *Consuelo* SO₂ transport pixels using the different emission data sets.
 3

	B. burning (GFED SO ₂)	Regional volcanic and strong anthropogenic (OMI SO ₂)	Volcanic (Aerocom SO ₂)	Anthropogenic (EDGAR SO ₂)
a) Pixel <i>El Tiro</i>				
B. burning (GFED SO ₂)	1			
Regional volcanic and strong anthropogenic (OMI SO ₂)	0.01	1		
Volcanic (Aerocom SO ₂)	0.14	0.42***	1	
Anthropogenic (EDGAR SO ₂)	-0.29*	0.52***	0.66***	1
b) Pixel <i>Cerro del C.</i>				
B. burning (GFED SO ₂)	1			
Regional volcanic and strong anthropogenic (OMI SO ₂)	-0.13	1		
Volcanic (Aerocom SO ₂)	0.13	0.60***	1	
Anthropogenic (EDGAR SO ₂)	-0.35**	0.69***	0.76***	1

4 Note. *** $p < 0.001$, ** $p < 0.01$, * $p < 0.05$.

1 Table 3: Cross-correlation matrix for SO₂ transport concentrations above *El Tiro* and *Cerro del*
 2 *Consuelo* pixels and sulfate concentrations from MSs of these two sites, located on a mountain
 3 pass upriver and on the highest catchment peak, respectively. Variables in bold represent
 4 measured sulfate (SO₄⁻) concentrations and non-bold variables SO₂ transport. OP stands for
 5 occult precipitation.
 6

	B. burning (GFED SO ₂)	Regional volcanic and strong anthropogenic (OMI SO ₂)	Volcanic (Aerocom SO ₂)	Anthropogenic (EDGAR SO ₂)
OP SO₄⁻ (<i>El Tiro</i>)	0.43***	0.40**	0.18	0.19
Rain SO₄⁻ (<i>El Tiro</i>)	0.08	0.33*	0.39**	0.46***
OP SO₄⁻ (<i>C. del Consuelo</i>)	0.27	0.43**	0.52***	0.37**
Rain SO₄⁻ (<i>C. del Consuelo</i>)	0.21	0.09	0.12	0.14

7 *Note.* *** $p < 0.001$, ** $p < 0.01$, * $p < 0.05$.

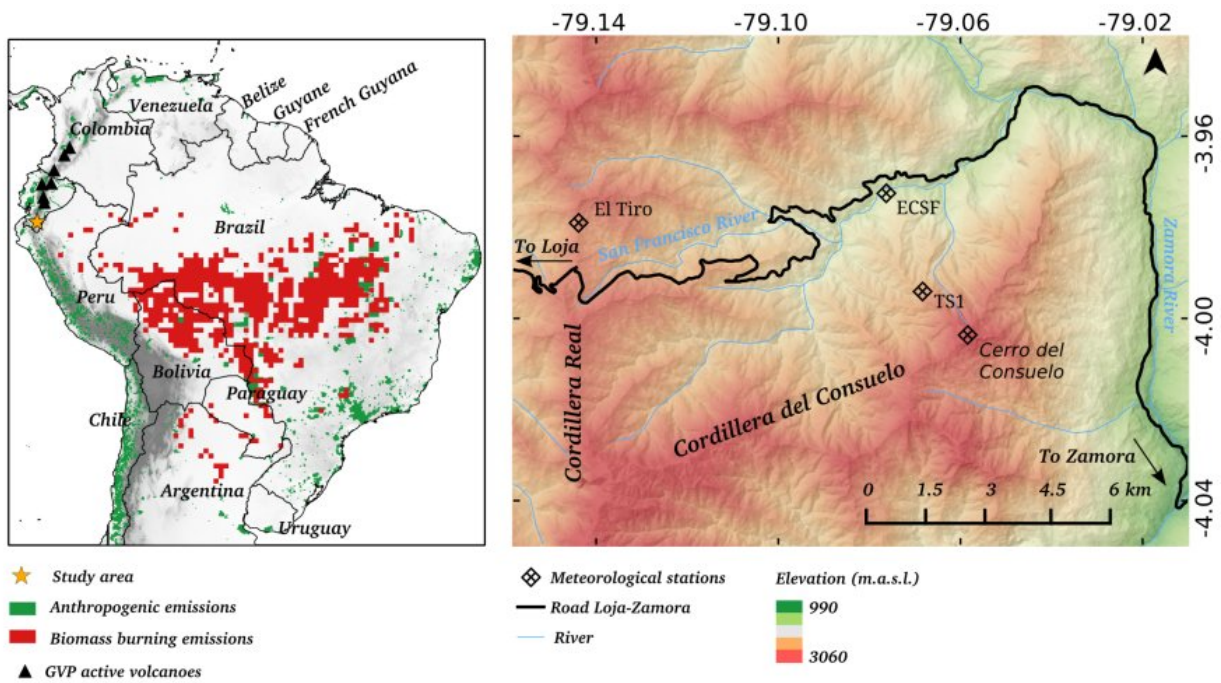
1 Table 4: Eigenvectors and communalities from factor analysis with varimax rotation, where a)
 2 shows the results of the data aggregated according to *Cerro del Consuelo* MS sample collection
 3 dates and b) those for *El Tiro* MS.

a)						
Eigenvectors						
	Factor 1	Factor 2	Factor 3	Factor 4	Factor 5	Factor 6
GFED SO₂	0.14	0.61	0.69	0.12	0.28	0.12
OMI SO₂	-0.48	-0.08	0.27	0.65	-0.40	-0.31
Aerocom SO₂	-0.51	-0.07	0.16	-0.44	0.46	-0.55
EDGAR SO₂	-0.53	-0.21	-0.02	0.17	0.39	0.70
Cerro del C. OP SO₄⁻	-0.42	0.41	-0.005	-0.5	-0.58	0.25
Cerro del C. rain SO₄⁻	-0.16	0.63	-0.64	0.30	0.23	-0.16
Communalities						
GFED SO₂	6%	55%	35%	1%	3%	0%
OMI SO₂	66%	1%	5%	19%	6%	1%
Aerocom SO₂	76%	1%	2%	9%	8%	5%
EDGAR SO₂	79%	6%	0%	1%	6%	8%

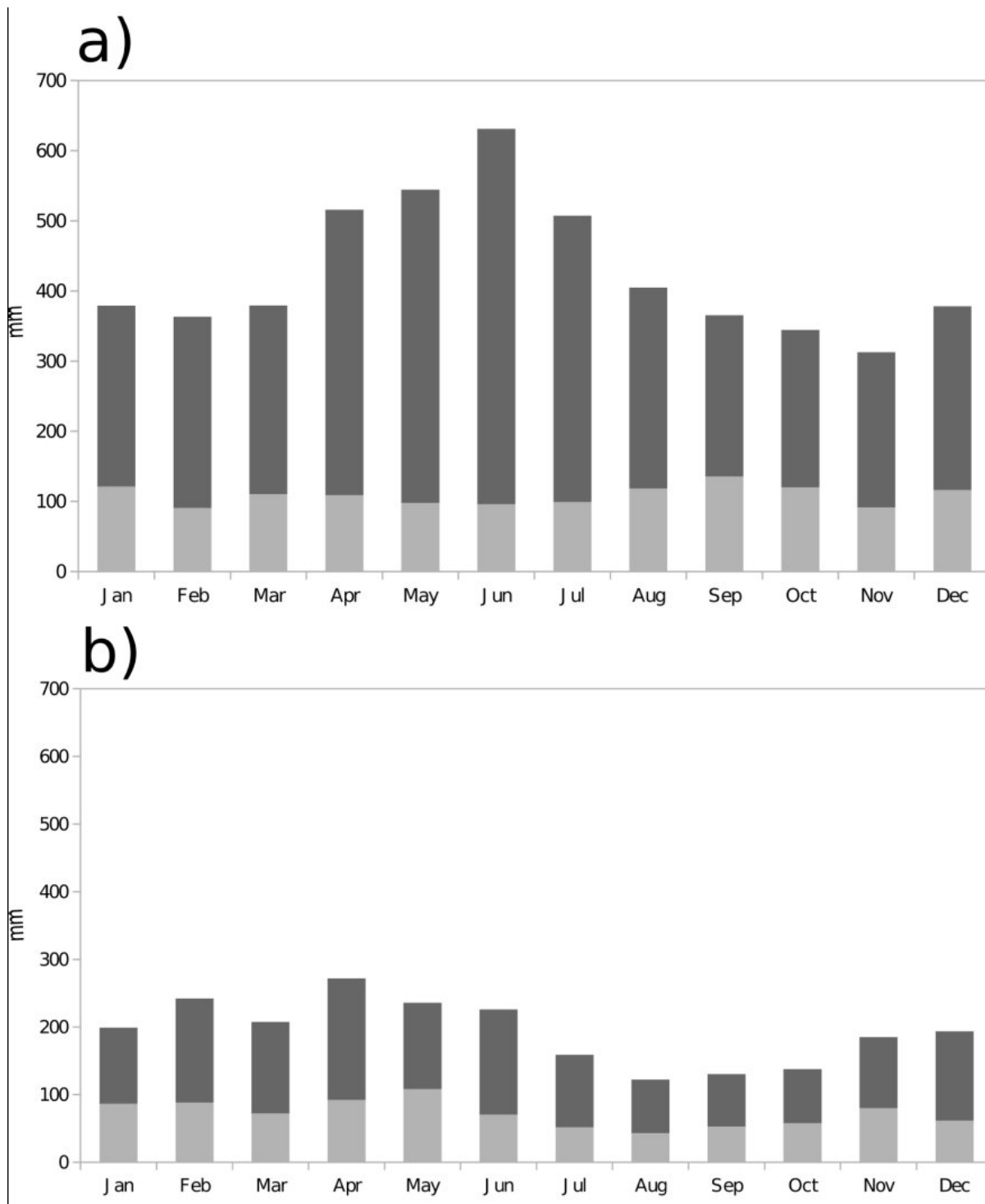
Cerro del C. OP SO₄⁻	50%	25%	0%	11%	13%	1%
Cerro del C. rain SO₄⁻	7%	56%	30%	4%	2%	0%

b)

Eigenvectors						
GFED SO₂	0.04	0.69	0.24	0.51	0.45	0.01
OMI SO₂	-0.47	0.1	-0.68	0	0.24	0.50
Aerocom SO₂	-0.47	-0.25	0.25	0.64	-0.46	0.17
EDGAR SO₂	-0.5	-0.33	0.02	0.03	0.52	0.60
El Tiro OP SO₄⁻	-0.34	0.56	-0.22	-0.18	-0.5	-0.48
El Tiro OP SO₄⁻	-0.44	0.16	0.61	0.08	-0.53	0.34
Communalities						
GFED SO₂	0%	75%	4%	14%	7%	0%
OMI SO₂	56%	1%	34%	0%	2%	7%
Aerocom SO₂	56%	10%	5%	22%	7%	1%
EDGAR SO₂	64%	17%	0%	0%	9%	10%
El Tiro OP SO₄⁻	30%	50%	4%	2%	8%	6%
El Tiro rain SO₄⁻	50%	4%	28%	15%	0%	3%

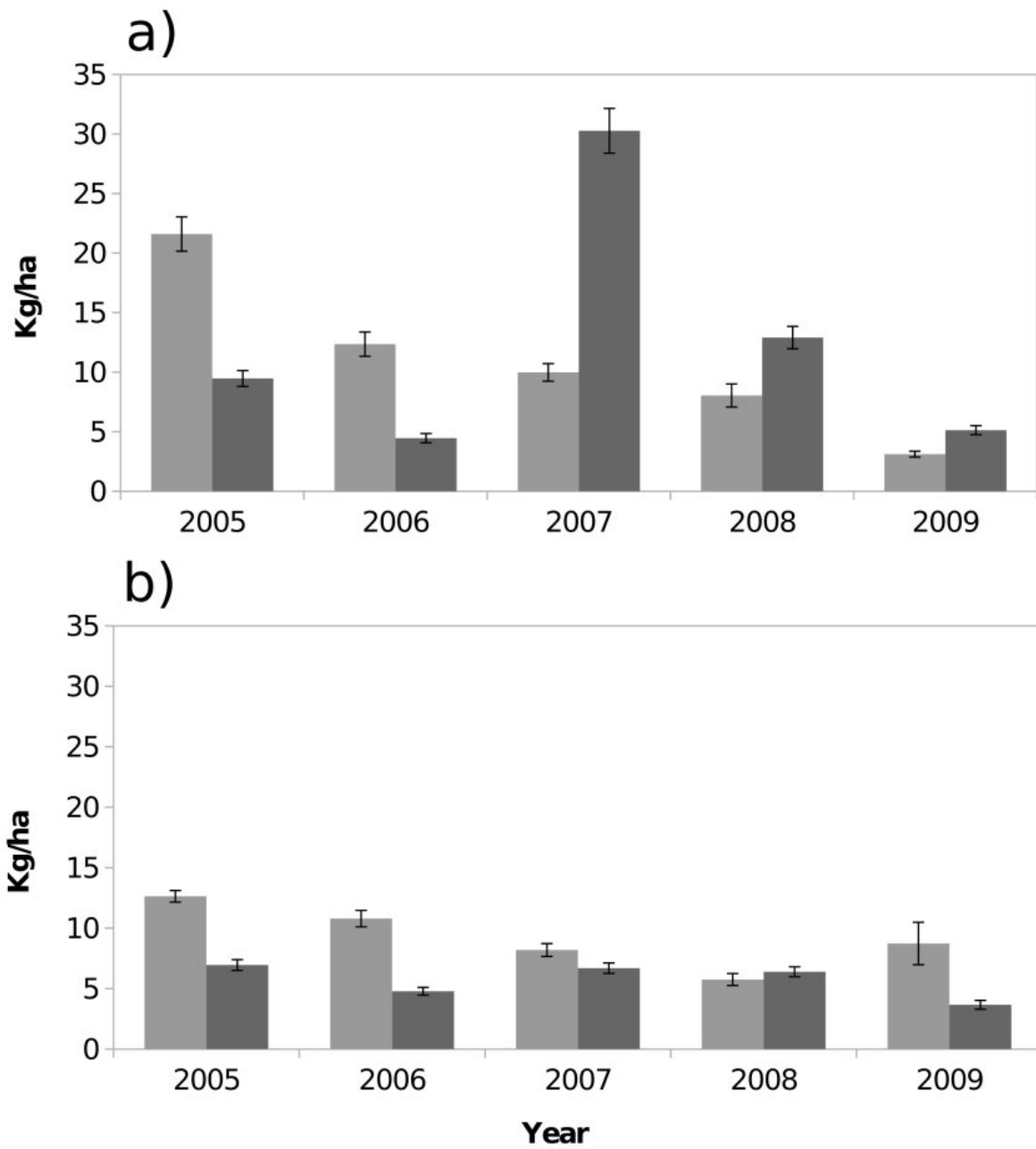


2 Figure 1: Study area. The left map shows possible anthropogenic and biomass-burning SO₂
 3 sources in tropical South America and the location of active volcanoes in Ecuador and Colombia.
 4 The right map depicts the study area in the River San Francisco catchment and the location of the
 5 meteorological stations (MSs) involved in the study.



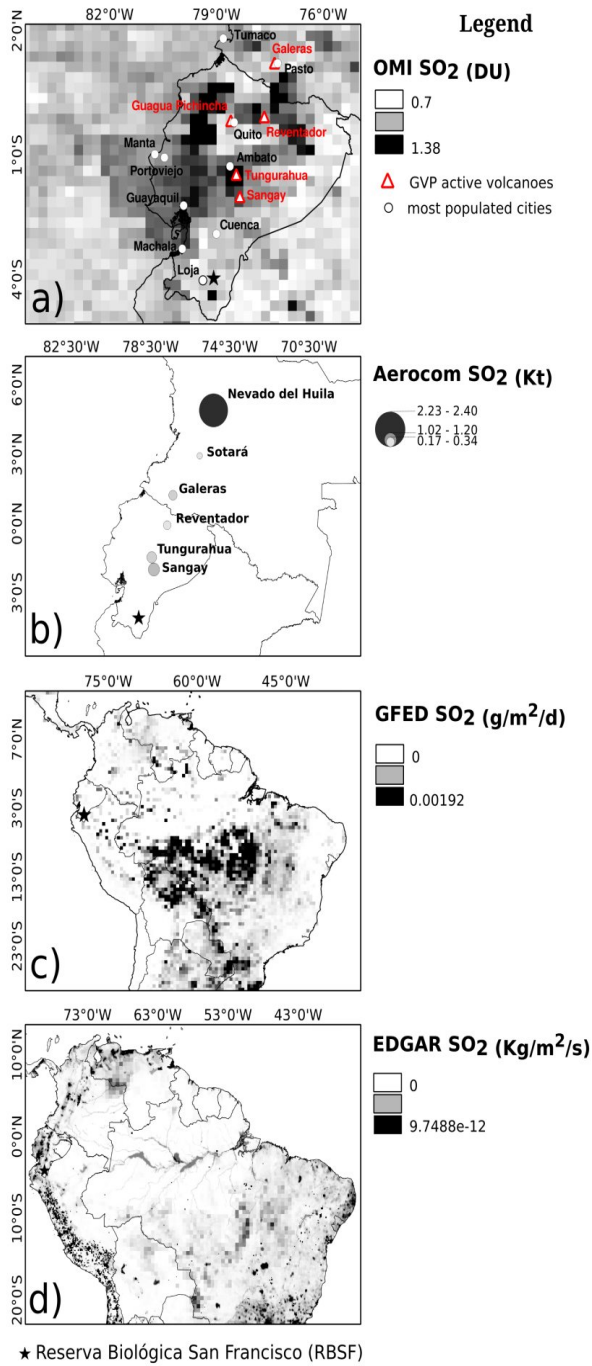
2 Figure 2: Rain (dark grey) and Occult Precipitation (OP) (light grey) monthly means for a) *Cerro*
 3 *del Consuelo* and b) *El Tiro* Meteorological Stations (MSs).

4

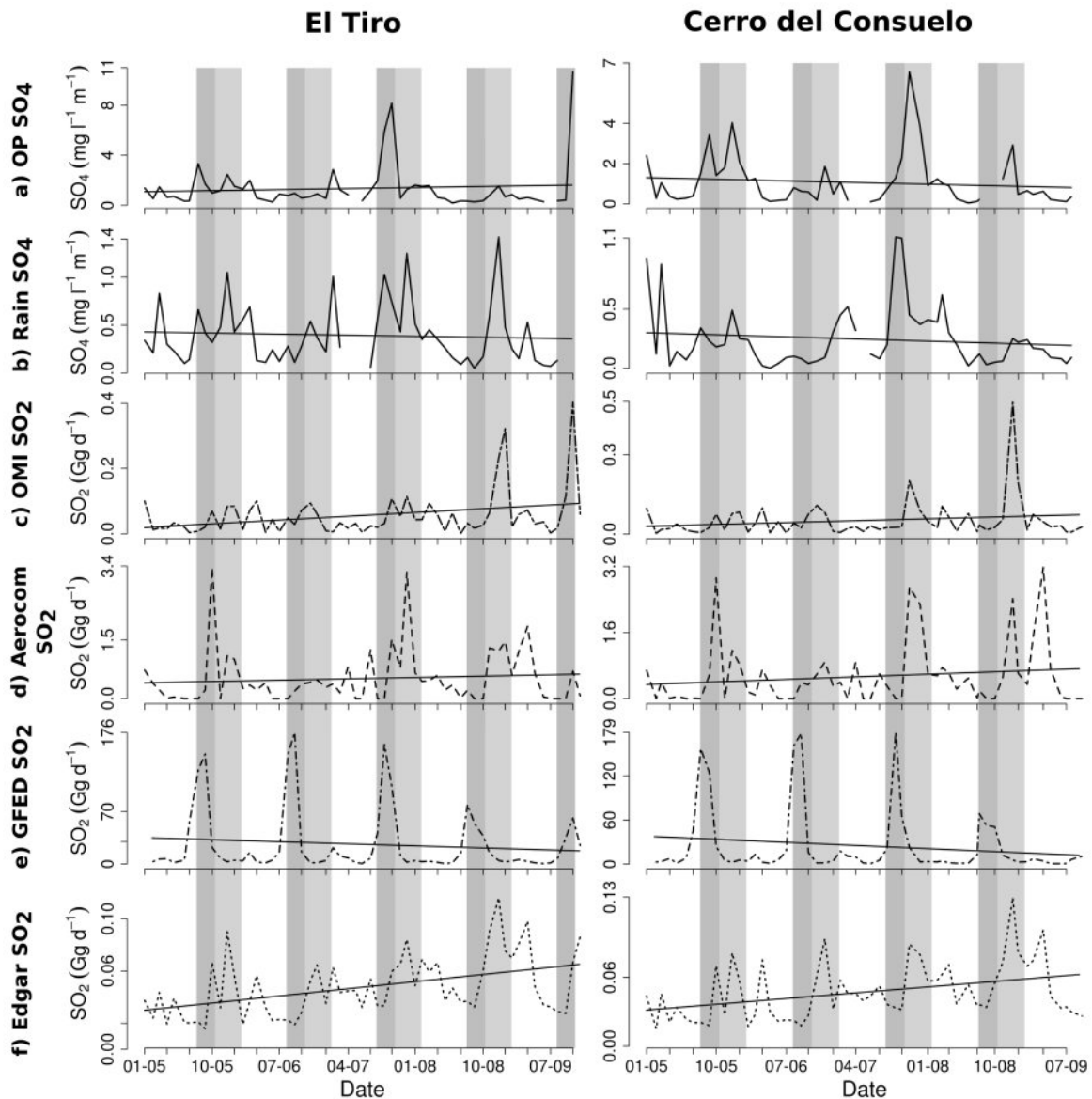


2 Figure 3: Total yearly sulfate (SO_4^-) deposition at a) *Cerro del Consuelo* and b) *El Tiro* MSs.
 3 Dark grey bars represent deposition by rain and light grey bars deposition by occult precipitation
 4 (OP).

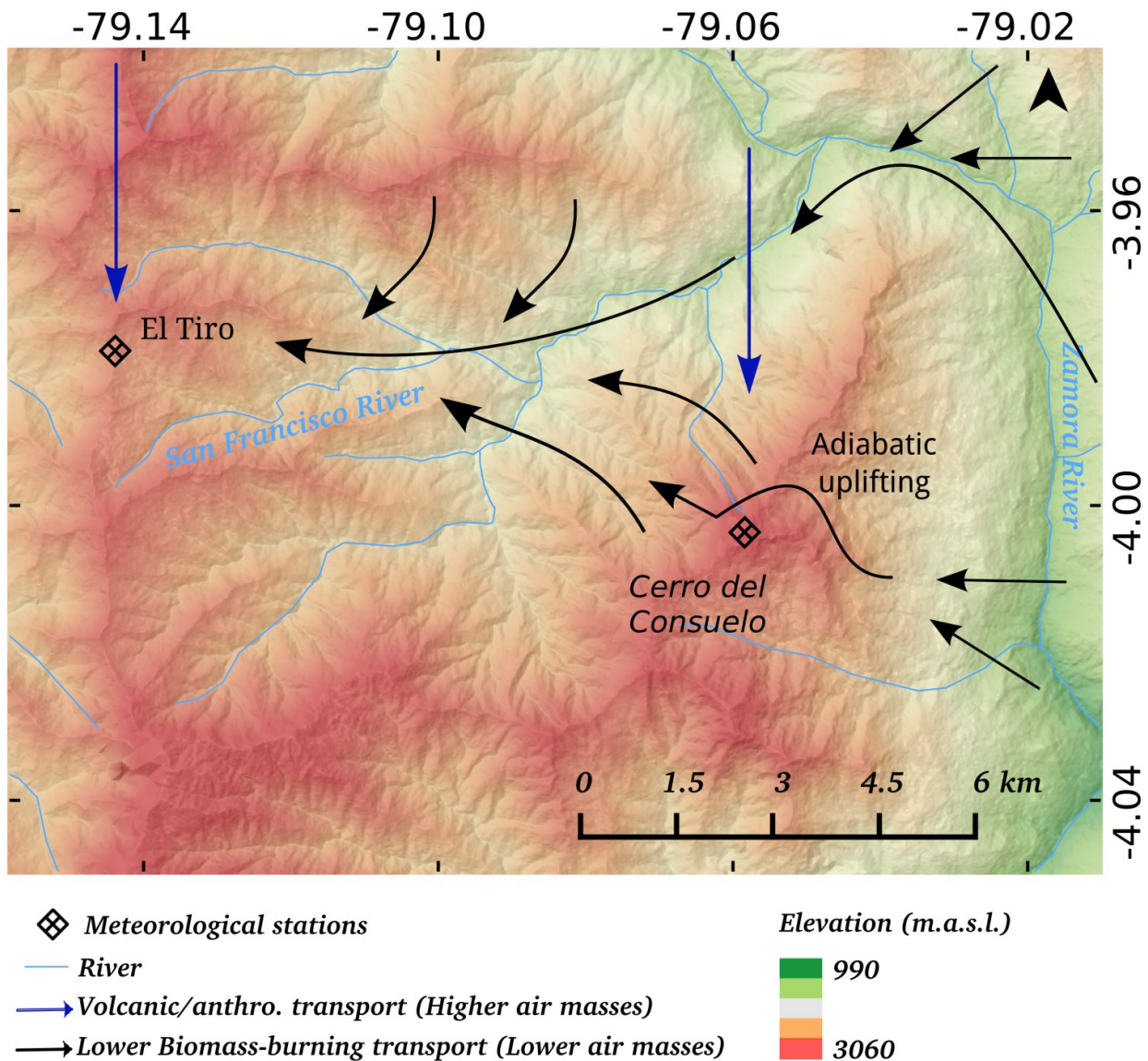
5
 6



2 Figure 4: Average 2005-2009 source-dependent emission maps for (a) volcanic and strong
 3 anthropogenic regional emissions, (b) volcanic eruptive and passive degassing, (c) biomass-
 4 burning, and (d) anthropogenic emissions.



2 Figure 5: Time series comparing SO₂ transport from (c) volcanic and strong anthropogenic
 3 regional emissions (OMI), (d) volcanic emissions (Aerocom), (e) biomass-burning (GFED), and
 4 (f) anthropogenic emissions (EDGAR), to measured sulfate concentrations in (a) occult
 5 precipitation (OP) and (b) rain water from *Cerro del Consuelo* (right panel) and *El Tiro* (left
 6 panel) Meteorological Stations (Mss). The black straight line represents the tendency. Dark grey
 7 bars depict the Amazonian biomass-burning season (easterly wind direction) and light grey bars
 8 the shift of the incoming air masses to a northerly-northwesterly-westerly direction. Note the
 9 different scaling of the y-axes.



2 Figure 6: Conceptual sketch of the deposition regimes observed in the study area. The blue
 3 arrows represent volcanic and anthropogenic transport from the north and north-west creating
 4 rain deposition at *El Tiro* Meteorological Station (MS) and Occult Precipitation (OP) deposition
 5 at *Cerro del Consuelo* MS. The black arrows represent biomass-burning transport from the east
 6 creating OP deposition at *El Tiro* MS and mainly rain deposition at *Cerro del Consuelo* MS.